Journal of Mining and Earth Sciences

Website: http://jmes.humg.edu.vn

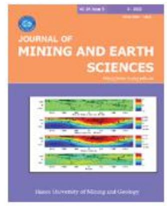

Some applications of Scanning Electron Microscopy to the study of reservoir rock

Luc The Trinh [1,2*], Tuan Van Pham [1], Bui Hoang Bac [1,2], Ngan Thi Bui [1], Hong Minh Thi Nguyen [1], Muoi Duy Nguyen [1], Hang Thu Thi Nguyen [1]

[1] *Hanoi University of Mining and Geology, Hanoi, Vietnam*
[2] *HiTech-CEAE Research Team, Hanoi University of Mining and Geology, Hanoi, Vietnam*

ARTICLE INFO

Article history:
Received 30th Jan. 2023
Revised 30th May 2023
Accepted 26th Jun. 2023

Keywords:
BSE,
EDS – Mapping,
Reservoir,
SEM,
SEM – EDS.

ABSTRACT

Scanning electron microscopy (SEM) is a powerful tool for visualising reservoir pore and grain framework systems which (SEM) provides qualitative information about pore geometry through direct observation of a rock or a pore cast of the rock. This aids in understanding reservoir productivity capabilities. The SEM is useful for locating and identifying minerals, particularly clay minerals - an aid when designing drilling and completion programs. SEM unlike conventional light microscopy, produces images by recording various signals resulting from interactions of an electron beam with the sample as it is scanned in a raster pattern across the sample surface. Combined with a backscatter detector (BSE), energy dispersal X-ray spectroscopy (EDS), and EDS - Mapping, SEM can yield multiple types of information about geological samples at the same time, such as superficial microstructure, BSE image, component analysis, and crystal structure features. In addition, new technic of SEM like Qemscan and FIB (Focused ion beam) can automatically minerals mapping and approach to 3-D imaging. In this paper, we use granite rock from a granitic basement reservoir, Bach Ho Oilfield as examples to discuss the geological application of SEM. The most important reservoir properties of granite rock in the oilfield are porosity and fractured pores which are abundant. The fractures have various sizes from mm to micron in width. Some large cracks have 1÷3 cm in lenght and 100÷600 μm in width. The small ones have 0.001÷0.2 mm in length and 10÷100 μm in width. Some large fractures were porefilled by crystals that have blade shape.

1. Introduction

Scanning electron microscopy is used extensively to provide qualitative information about the pore geometry of rocks, either directly or indirectly through the examination of pore casts. Many of these studies were concerned with relating pore geometry to various tests or rock properties; specific applications also are discussed. The basic principles of the SEM were known in 1935 (Knoll and Max, 1935). The SEM provides several unique advantages for geologists

*Corresponding author
E - mail: trinhtheluc@humg.edu.vn
DOI: 10.46326/JMES.2023.64(3).04

or engineers in comparison with other types of microscopes:

Magnification range of 15 x to a practical upper limit of about 50,000 x for rocks;

Great depth of field (closest focus point to furthest focus point is large);

Ease of sample preparation - samples made conductive by a coating of metal applied under vacuum, nondestructive sample study;

Useful for locating and identifying minerals, particularly clay minerals.

A two dimension (2D) image is produced in SEM by detecting the interaction of the surface of a specimen and an electron beam, this interaction produces a range of signals which are detected by the detector and imaged a 2D image (Reimer, 2000; Goldstein et al., 2012). Electrons bounced back out of the sample are recognised as backscattered electrons (BSE) while these knocking into the sample with the displacement of atoms are called secondary electrons (SE). The interaction volume involved in the production of SE, BSE, and X-rays can vary with the change of the accelerating voltage, aperture, and spot size of the beam as well as the landing energy, the atomic number of the sample and the density of the sample and it generally forms as a teardrop to a semi-circle within the specimen. The amount of backscattered electrons is determined by the atomic number of the specimen, and consequently, BSE images are mainly used to demonstrate compositional contrasts within a sample and also suggest the average atomic number of the sample. The difference between BSE and SE images is that SE images show texture and topography as more secondary electrons can be captured from the edges and sharps, which are looked brighter and showed more details than other areas. Figure 1 demonstrates the interaction volume of the specimen and electron beam in the SEM imaging procedure.

2. Method

Sample Preparation: a granodiorite core at 4,117 m depth from Bach Ho oilfield was cut into pieces measuring around 3x1 cm (radius × thickness) by using a diamond saw; then samples were processed for grinding and polishing. Each sample was attached to the SEM stub using a carbon adhesive tab and then coated with carbon to give better conductivity.

Experiment Operation: Investigation was performed by using a scan electron microscope with EDS (Figure 2) (Model: Quanta 450; Produced by: FEI-USA) at the Center for Excellence in Analysis and Experiment - Hanoi University of Mining and Geology. In the experiments, we used a high acceleration voltage

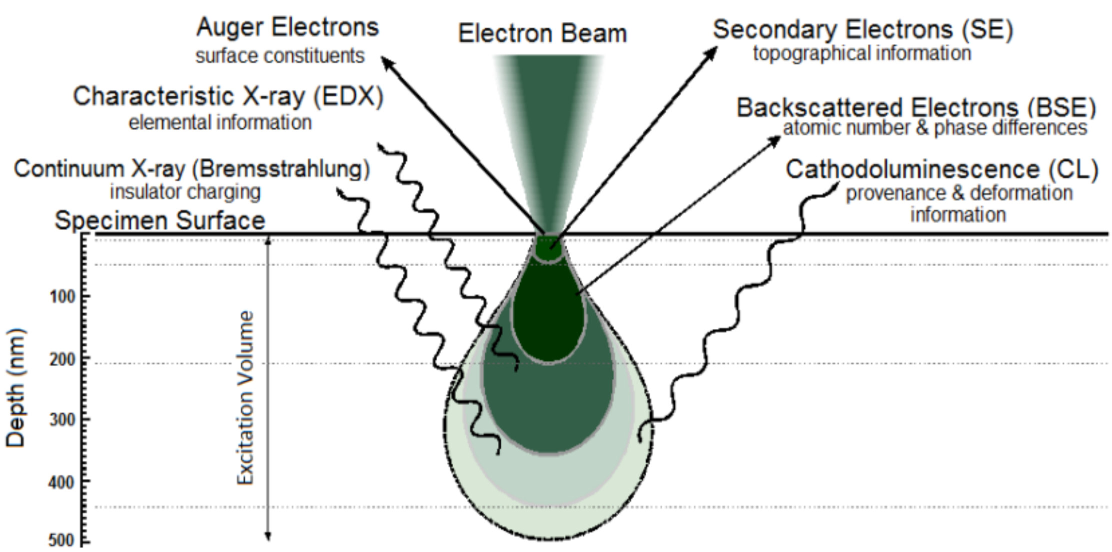

Figure 1. Interaction Volume of sample surface and electron beam during SEM imaging with various signals produced (Salh, 2011).

Figure 2. Quanta 450; Produced by: FEI-USA.

of 20 kV, with a working distance of 10 mm and magnification of 100÷50,000.

Lower magnification is always used to get general information of overlook on sample surface whereas higher magnification gave more details of features found on the samples. Both secondary electron and backscattered electron detectors were applied in this study, and an energy dispersive spectroscope (EDS) system equipped with SEM was introduced to form element mapping.

3. Results and Discussion

3.1. Structure analysis by BSE (Backscattered electrons)

In SEM investigation, pores could be classified into 3 groups: interparticle pores (interP pores), intraparticle pores (intraP pores) and fracture pores (frt pores). This classification has been recommended in many previous studies and has been used widely (Loucks et al., 2009; Loucks et al., 2010; Fishman et al., 2012; Milliken et al., 2012). Interparticle pores can be found in the area with quartz, feldspar K, pyrite or other crystals. Intraparticle pores are usually found within pyrite framboids (between individual crystals) muscovite and Intra feldspar K crystals (Figure 3).

Based on the SEM investigation of this sample, we find that it is better to recognize and group the pores into two general types according to their sizes: micropores (pores with diameters >1 μm) and nanopores (pores having the diameters <1 μm). In this sample, nanopores are the Intraparticle pores whereas micropores show more appearance around or in pyrite, quartz and feldspar K. Fracture pores are the most common pores in several sizes, some of them were filled with secondary crystals. The group of interparticle pores have greater sizes with micropores are of 2 to 8 μm in diameter. Intraparticle pores are usually found within and along cleavage planes in micaceous grains and are typically very small pores (nanopores) in quartz and feldsparK grains. Interparticle pores are

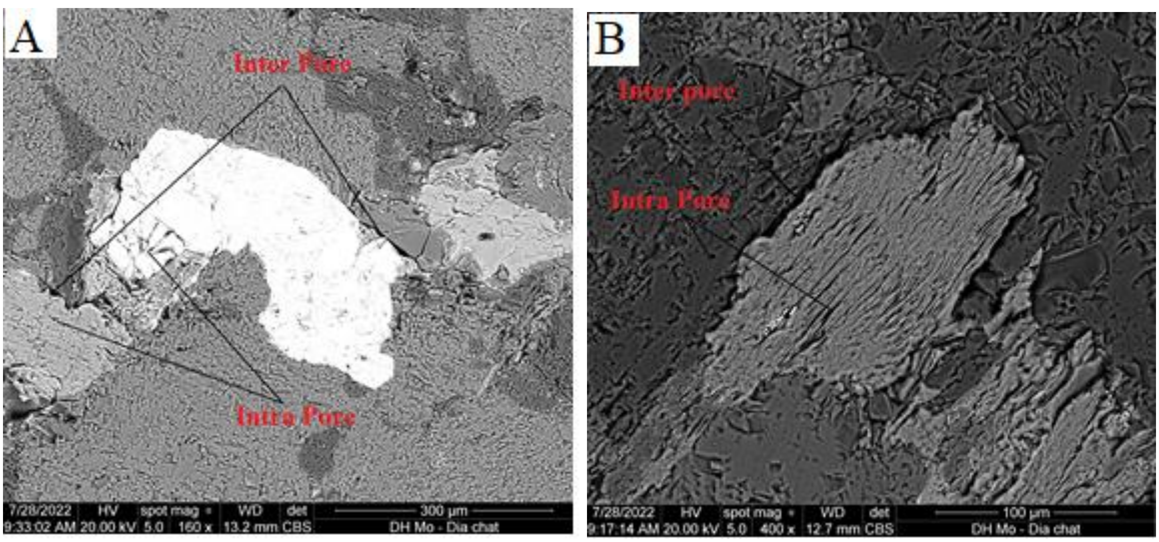

Figure 3. SEM Images of Granite Pore Types A: Intraparticle pores found within pyrite framboid, interparticle pores surrounded pyrite and muscovite pores along pyrite particles. B: interparticle pores between muscovite and feldspar K and in between feldspar K, Quartz crystal.

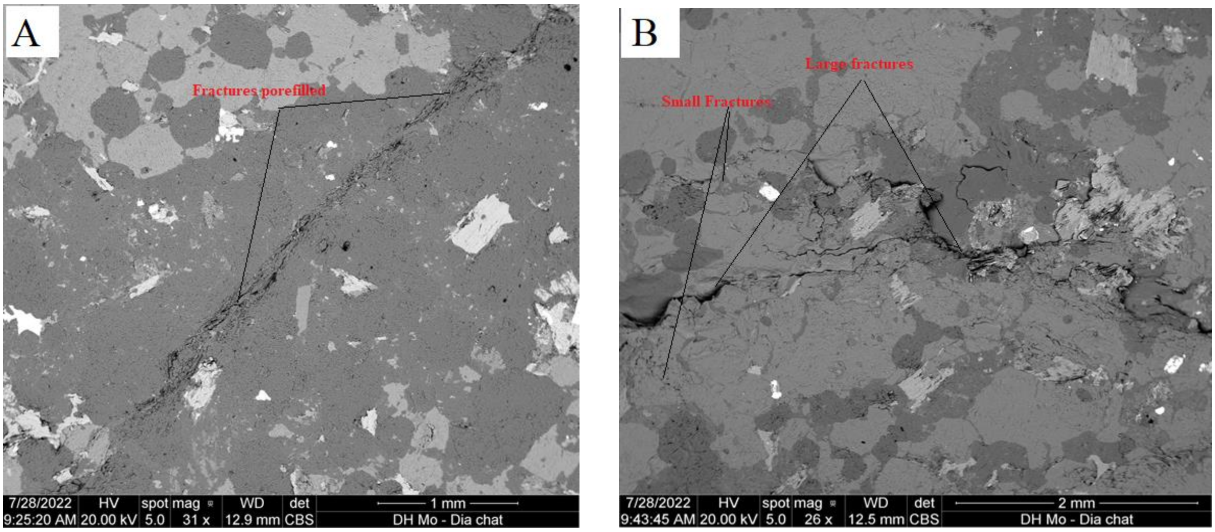

Figure 4. SEM Images of Granite Pore Types A: Large Porefilled fractures; B: Fractures system.

commonly observed at the margins of large grains. The size of nano to micro-intercrystalline pores associated with quartz and feldspar K. Pores with a size of around 200 nm are usually found within small framboids (300÷500 nm in size).

The most abundant pores in Bach Ho granite are fractured pores. Fractures in this sample have various sizes from mm to micron in width. Some large cracks have 1÷3 cm in length and 100÷600 μm in width. The small cracks have 0.001÷0.2 mm in length and 10÷100 μm in width (Figure 4). Some large fractures have been porefilled by crystals that have blade shape.

3.2. Mineralogy (EDS: Energy-dispersive X-ray spectroscopy)

To better investigate the materials and identify the mineral composition, EDS system within SEM was introduced. Several certain areas were chosen for element identification by SEM - EDS as shown in Figure 5. The EDS results prove the existence of rock-forming minerals: quartz, feldspar K, mica, and ore minerals mostly pyrite and little zircon.

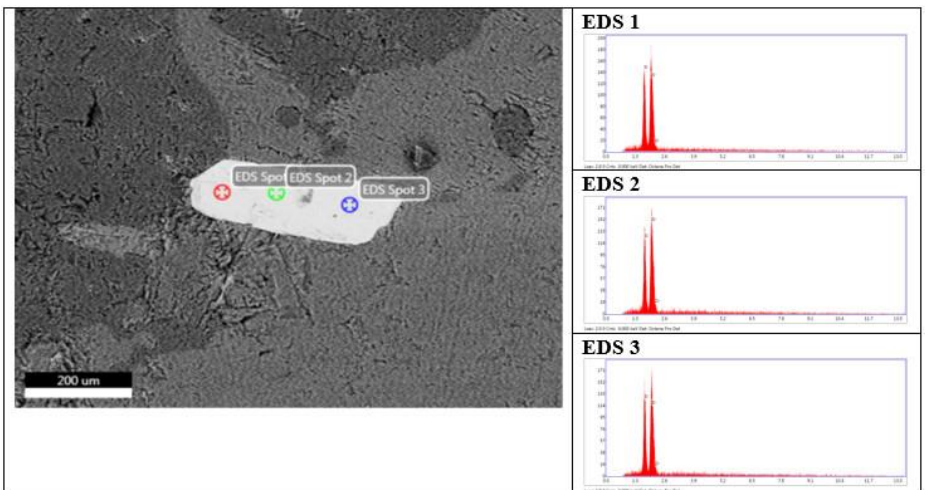

Element component

Element	Si	Zr	Oxygen
Average Percentage (%)	9.52	27.97	0.45
Equation	$ZrSiO_4$		Zircon

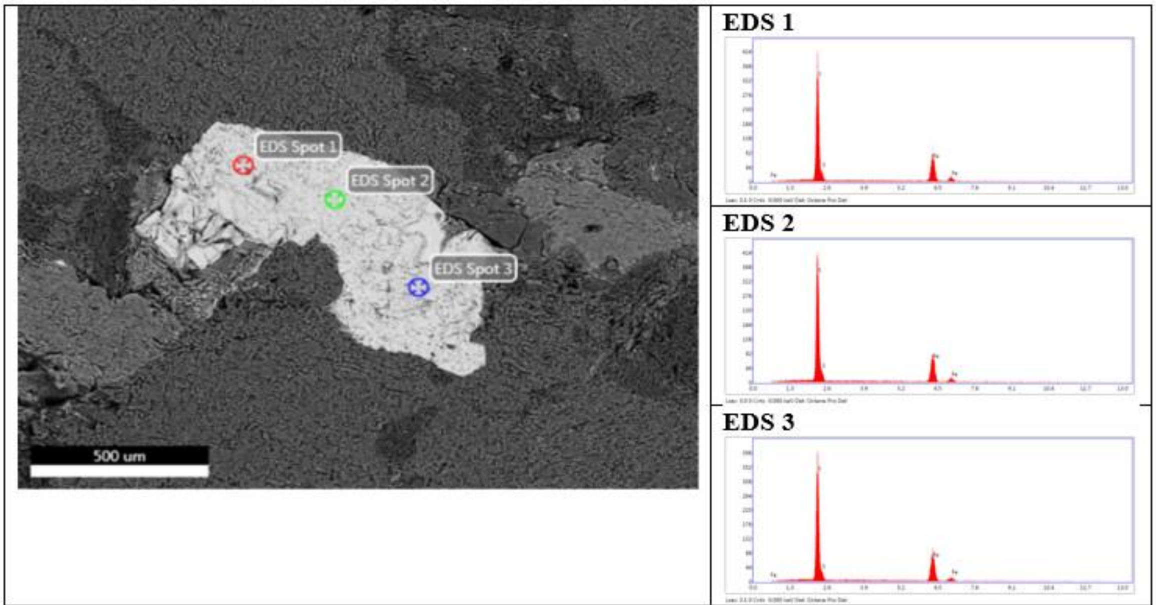

Element component

Element	S	Fe
Average Percentage (%)	50.11	49.88
Equation	FeS	**Pyrite**

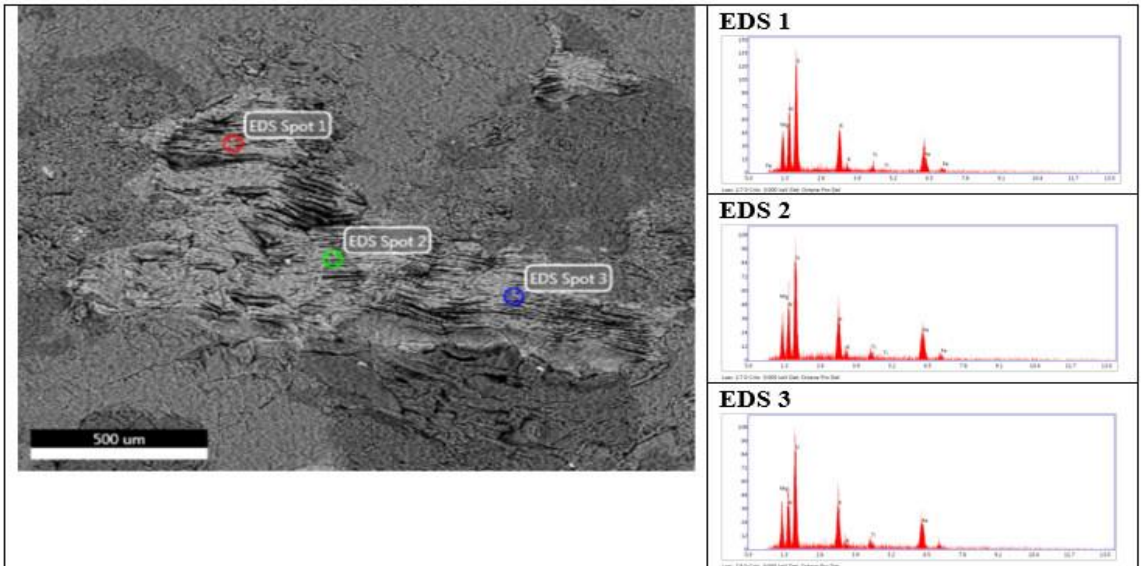

Element component

Element	Mg	Al	Si	K	Ti	Fe
Average Percentage (%)	8.50	13.93	28.79	16.18	2.80	29.81
Equation	$K(MgFe)_3(AlSi_3O_{10})(F,OH)$				**Biotite**	

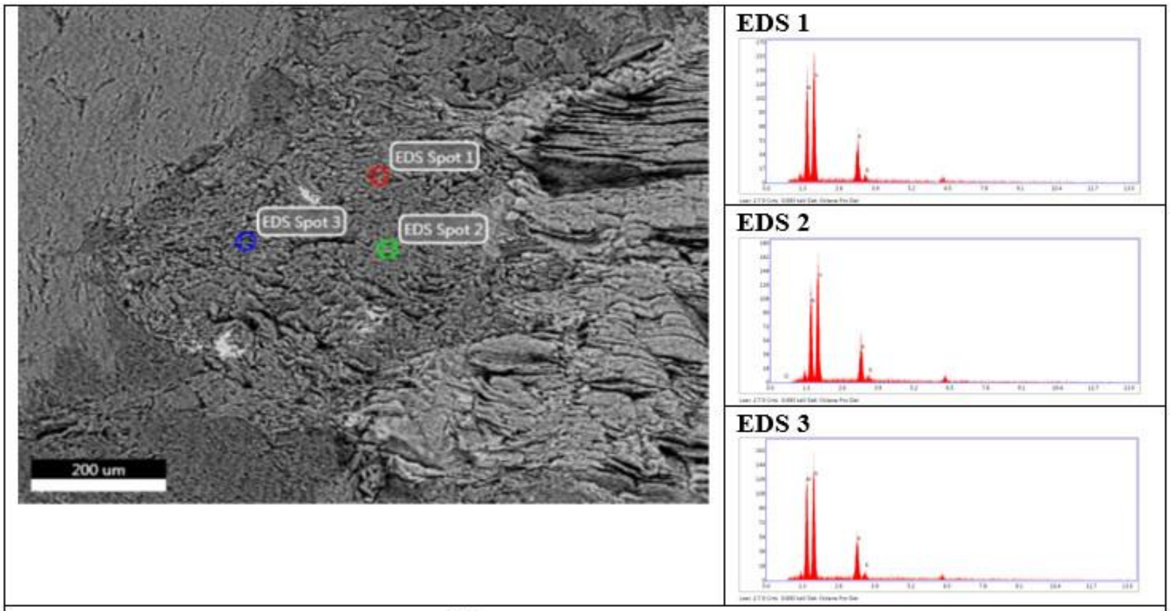

Element component

Element	Al	Si	K
Average Percentage	13.93	28.79	16.18
Equation	$KAl_2(AlSi_3O_{10})(F,OH)$		Muscovite

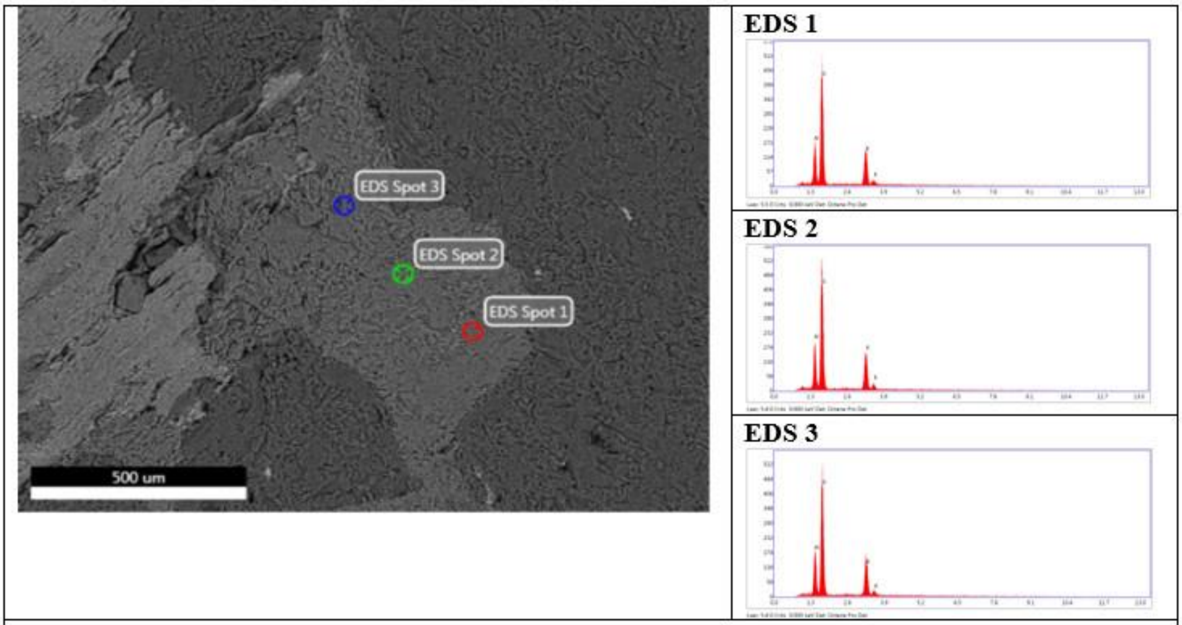

Element component

Element	Al	Si	K
Average Percentage (%)	14.84	53.93	31.23
Equation	$KAl_{1,4}Si_{3,3}O_8$		Feldspar K

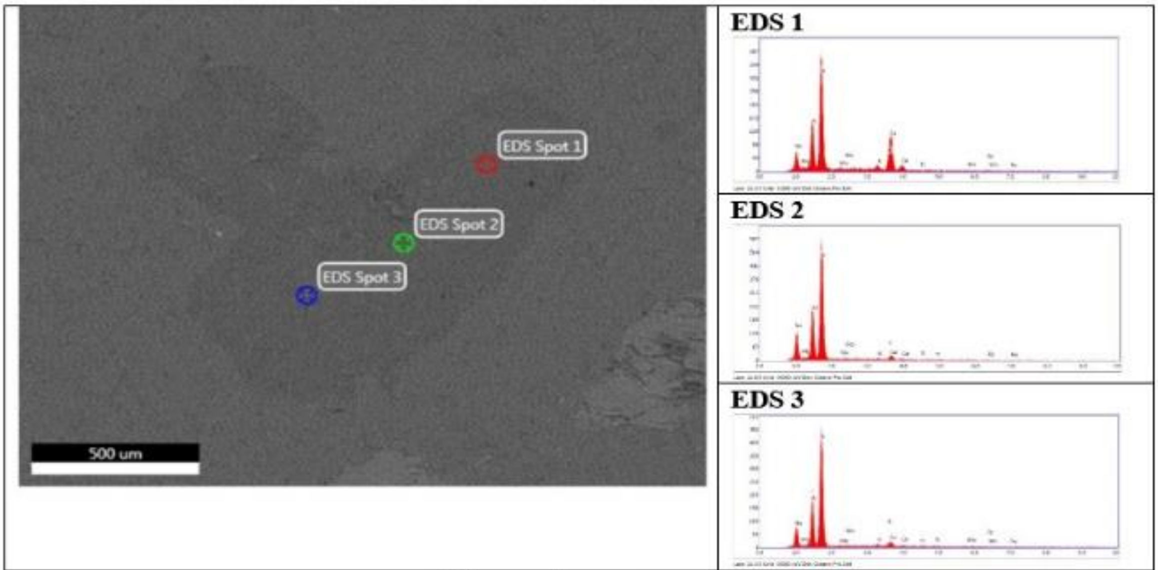

Element component

Element	Na	Al	Si	Ca
Average Percentage (%)	9.1	18	50.84	14.15
Equation	$Ca_{0.93}$ $NaAlSi_3O_8$			Andesine

Figure 5. Mineral identification by SEM – EDS.

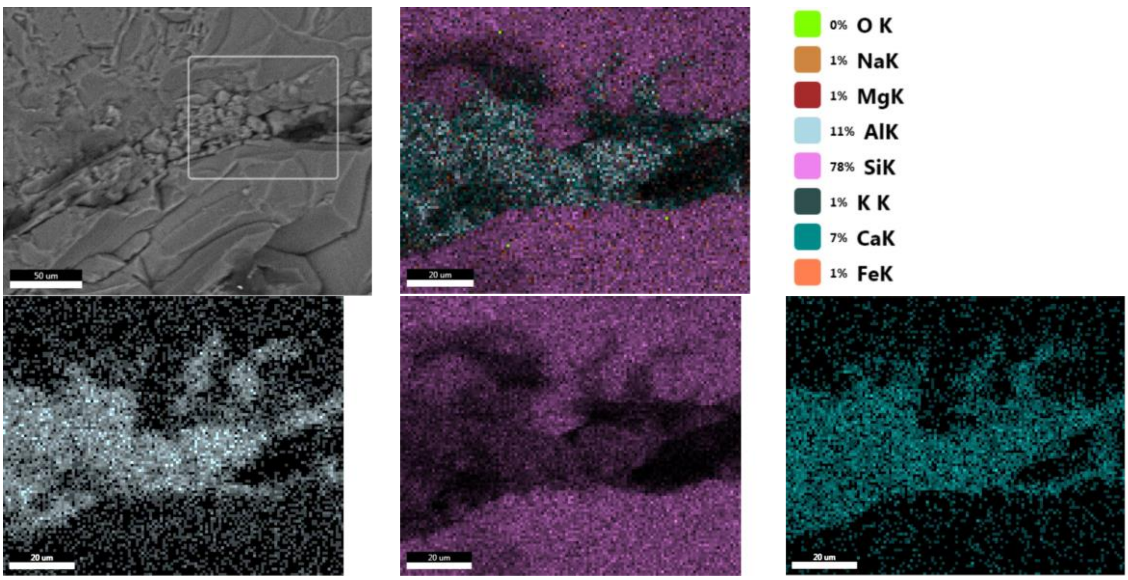

Figure 6. EDS mapping of fracture area showed the elements dyke on fracture.

3.3. Element mapping (EDS - Mapping)

EDS - Mapping is used to identify elements in fracture pores (Figure 6). For the determination of porosity, the "Pores" were determined using a custom classification, in which material that had a greyscale of a certain range was scripted to be "Pores" instead of background material. This darker material of "Pores" was not matched to any X-ray standard. The results for the individual area were acquired as a digital EDS map of the elements and a data table listing their composition.

The composition of a mineral was identified based on Energy-dispersive X-ray spectroscopy (EDS) (Figure 6). Fractures have been filled with Ca ($CaCO_3$) and Si, Al (Clay). Pores appeared with micro size (dark part).

The pores System of the sample could be visualization of the pore network and rock fabric architecture by FIB/SEM (Lemmens, et al., 2011; Goral, et al., 2015). The FIB-SEM technique relies on using a FIB to polish away a thin (~10 nm) layer of material and having a resolution of a few nanometers in the section plane. A high-resolution feld-emission SEM is used to image the structure and then repeated to the full area of the sample which gives a serial sectioning approach to 3-D imaging.

4. Conclusion

Scanning electron microscopy provides different modes and techniques for acquiring high-quality images of granite and other rock samples. The images in this chapter demonstrate their fine resolution and their applicability for the characterization of granite reservoirs

Bach Ho field is unusual in that the fractured reservoir matrix is largely made up of unaltered acid igneous lithologies and the pore system of that is dominated by fracture pores. Fracture pores play a main role in contain and also transporting petroleum.

The most abundant pores in Bach Ho granite are fractured pores. The fractures have various sizes from mm to micron in width. Some large cracks have 1÷3 cm in lenght and 100÷600 μm in width. The small cracks have 0.001÷0.2 mm in lenght and 10÷100 μm in width. Some large fractures were porefilled by crystals that have blade shape.

The recent emerging shale and granite oil and gas exploration requires state-of-art imaging and characterization techniques to study the application of clay minerals in the exploration of this unconventional resource. The up-to-date innovative FIB/SEM/EDS have been playing key roles in the identification and quantitative characterization of minerals, which help define the best brittle reservoir intervals and avoid exploration failure by choosing compatible drilling and hydraulic fluids.

Acknowledgments

This paper was supported by the Department of Petroleum Geology and the Center for Excellence in Analysis and Experiment (HUMG) and was supported with funding from the science and technology project T22-13 of Hanoi University of Mining and Geology.

Contribution of authors

Luc The Trinh: Conceptualization, Formal analysis, Funding acquisition, Investigation, Writing-review & editing; Bui Hoang Bac: Formal analysis, Investigation; Tuan Van Pham: Methodology, Formal analysis, Investigation, Writing-review & editing; Hang Thi Nguyen: Formal analysis; Ngan Thi Bui: Funding acquisition, Writing-review & editing; Muoi Duy Nguyen: Investigation; Hong Minh Thi Nguyen: Methodology.

References

Fishman, N. S., Hackley, P. C., Lowers, H. A., Hill, R. J., Egenhoff, S. O., Eberl, D. D., & Blum, A. E. (2012). The nature of porosity in organic-rich mudstones of the Upper Jurassic Kimmeridge Clay Formation, North Sea, offshore United Kingdom. International Journal of Coal Geology, 103, 32-50.

Goldstein, J., D. E. Newbury, P. Echlin, D. C. Joy, A. D. Romig Jr, C. E. Lyman, C. Fiori and E. Lifshin (2012). Scanning electron microscopy and X-ray microanalysis: a text for biologists, materials scientists, and geologists, Springer Science & Business Media.

Goral, J., Miskovic, I., Gelb, J., & Andrew, M. (2015). Correlative XRM and FIB-SEM for (non) organic pore network modeling in Woodford shale rock matrix. In International Petroleum Technology Conference. OnePetro.

Knoll & Max M., (1935). Aufladepotentiel und Sekundäremission elektronenbestrahlter Körper. Zeitschrift für Technische Physik. 16: 467-475.

Lemmens, H. J., Butcher, A. R., & Botha, P. W. S. K. (2011). FIB/SEM and SEM/EDX: a New Dawn for the SEM in the Core Lab?. Petrophysics, 52(06), 452-456.

Loucks, R. G., Reed, R. M., Ruppel, S. C., & Jarvie, D. M. (2009). Morphology, genesis, and distribution of nanometer-scale pores in siliceous mudstones of the Mississippian Barnett Shale. Journal of sedimentary research, 79(12), 848-861.

Loucks, R. G., R. M. Reed, S. C. Ruppel and U. Hammes (2010). Preliminary classification of matrix pores in mudrocks. Gulf Coast Association of Geological Societies Transactions, v. 60, p. 435-441.

Milliken, Mark Rudnicki, David N. Awwiller, and Tongwei Zhang, (2012). Organic matter-hosted pore system, Marcellus Formation (Devonian), Pennsylvania. AAPG Bulletin, v. 97, no. 2 (February 2013), pp. 177-20.

Reimer, L. (2000). Scanning electron microscopy: physics of image formation and microanalysis. Measurement Science and Technology, 11(12), 1826-1826.

Salh, R. (2011). Silicon nanocluster in silicon dioxide: cathodoluminescence, energy dispersive X-ray analysis and infrared spectroscopy studies, INTECH Open Access Publisher.